Journal of Quantitative Spectroscopy & Radiative Transfer 109 (2008) 1060–1080

Journal of Quantitative Spectroscopy & Radiative Transfer

www.elsevier.com/locate/jqsrt

The sensitivity of radiative transfer calculations to the changes in the HITRAN database from 1982 to 2004

David P. Kratz*

Climate Science Branch, NASA Langley Research Center, Hampton, VA 23681-2199, USA

Received 16 August 2007; received in revised form 10 October 2007; accepted 23 October 2007

Abstract

Over the last quarter century, improvements in the determination of the spectroscopic characteristics of the infrared-active trace species have enhanced our ability to retrieve quantitative distributions of temperatures, clouds, and abundances for various trace species within the Earth's atmosphere. These improvements have also allowed for refinements in the estimates of climatic effects attributed to changes in the Earth's atmospheric composition. Modeling efforts, however, have frequently experienced significant delays in assimilating improved spectroscopic information. Such is the case for highly parameterized models, where considerable effort is typically required to incorporate any revisions. Thus, a line-by-line radiative transfer model has been used to investigate the magnitude of the effects resulting from modifications to the spectroscopic information. Calculations from this line-by-line model have demonstrated that recent modifications to the HITRAN (High Resolution Transmission) line parameters, the continuum formulation, and the CO_2 line-mixing formulation can significantly affect the interpretation of the high spectral resolution radiance and brightness temperature retrievals. For certain moderate-resolution satellite remote sensing channels, modifications to these spectroscopic parameters and formulations have shown the capacity to induce changes in the calculated radiances equivalent to brightness temperature differences of 1–2 K. Model calculations have further shown that modifications of the spectroscopic characteristics tend to have a modest effect on the determination of spectrally integrated radiances, fluxes, and radiative forcing estimates, with the largest differences being of order $1\,\mathrm{W\,m^{-2}}$ for the total thermal infrared fluxes, and of order 2–3% of the calculated radiative forcing at the tropopause attributed to the combined doubling of CO_2, N_2O, and CH_4. The results from this investigation are intended to function as a guide to differentiate between cases where older parameterizations provide acceptable results, within specified accuracy bounds, and cases where upgrades to the latest spectroscopic database are necessary.
Published by Elsevier Ltd.

Keywords: HITRAN database; Line parameters; Line-by-line calculation; Correlated *k*-distribution; Infrared; Radiances; Fluxes; Radiative forcings

*Tel.: +1 757 864 5669; fax: +1 757 864 7996.
E-mail address: david.p.kratz@nasa.gov

0022-4073/$ - see front matter Published by Elsevier Ltd.
doi:10.1016/j.jqsrt.2007.10.010

1. Introduction

Investigations based on radiative transfer calculations have established that natural and anthropogenic perturbations to the abundances of the infrared-active molecular species in the Earth's atmosphere are capable of producing radiative forcings that have the potential to significantly affect the climate. Indeed, the observed increases in the well-mixed greenhouse gases CO_2, CH_4, and N_2O force the climate to a warmer state [1] by augmenting the absorption and emission of radiation in the Earth's atmosphere through the excitation and relaxation of molecular pure-rotation and rotation–vibration transitions. Determining the accuracy of the radiative transfer calculations, however, remains crucial to improving our understanding of the radiative forcings and subsequent feedbacks resulting from changes to the composition of the Earth's atmosphere as well as other factors such as land use, vegetation cover, and solar insolation.

Currently, the monochromatic model is the most precise method available to calculate the radiative forcings of the infrared-active trace species. Also known as the line-by-line calculation, this method uses rigorous techniques to determine the complex relationship between the absorption coefficient and wave number, with sufficient spectral resolution to accurately compute the spectrum of absorption coefficients. Nearly two decades ago, the Inter-Comparison of Radiation Codes in Climate Models endeavor [2] established a fairly high degree of agreement among the participating monochromatic methods for broadband infrared cases. Nevertheless, this inter-comparison did not constrain the line-by-line calculations sufficiently to differentiate between the inherent physical differences within the algorithms and mere input and output choices. In a more carefully controlled inter-comparison experiment, Tjemkes et al. [3] demonstrated that the current line-by-line models agreed with one another over much of the mid-infrared from 800 to 2600 cm^{-1}. In addition, by using an empirically tuned water vapor continuum, the line-by-line models were further shown to agree with measured mid-infrared spectra to within observational accuracy. Shortly thereafter, in an inter-comparison of six distinct line-by-line models, Kratz et al. [4] demonstrated that, by strictly controlling model runs, remarkably good agreement among those six models could be achieved for the far-infrared (100–650 cm^{-1}) computations of both radiances and spectrally integrated radiances. While differences of order 0.5% were achieved for the radiance computations in the controlled runs, much larger differences in the radiances were encountered when the selection of molecular absorption bands, altitude integration methods [5–7], line parameter databases [8], and continuum absorption formulations [9,10] were not reconciled. Missing absorption bands and simplistic altitude integration schemes are most frequently issues that only afflict highly parameterized models. In contrast, the primary uncertainties associated with the line-by-line calculations tend to be related to the accuracy of spectroscopic parameters used to calculate the radiative effects of the infrared-active species, and the method used to treat the continuum absorption [11].

Since the publication of the 1982 AFGL (Air Force Geophysical Laboratory) line parameter database [12], five major editions [8,13–16] of the HITRAN (High Resolution Transmission) database have been released. Advancements in both theoretical quantum mechanical calculations and laboratory spectral measurements during this time have led to an overall improvement in the accuracy of the line parameters as well as a substantial increase in the number of reported transitions. To better understand the ramifications of the changes to the spectral databases, the present work focuses on the impact that improved line parameters have both on the low to moderate spectral resolution calculations used to estimate the climatic effects attributed to changes in the Earth's atmospheric composition [1], and on the moderate to high spectral resolution calculations used to retrieve atmospheric temperature profiles and trace gas abundances and distributions [17]. Section 2 provides a very brief review of the changes in the HITRAN database over the last quarter century. Then, after a brief summary of the model used in this study, attention is focused upon the impact that changes to the HITRAN database have upon the results from monochromatic calculations for the thermal infrared (0–3000 cm^{-1}). As will be demonstrated, care must be taken when interpreting the results, since modest changes between successive editions of the database do not imply the absence of significant changes in future editions. A case study will then be presented for the spectral intervals in the widely used Fu and Liou model [18], followed by a brief synopses concerning continuum formulations, line-mixing effects, and HITRAN database uncertainties. Concluding remarks are provided in Section 5.

2. Changes to the HITRAN infrared line parameters (1982–2004)

Reliable spectroscopic databases are absolutely essential for calculating accurate transmission spectra of radiatively active molecular species. Recognized as the international standard, the HITRAN database has been used for a wide variety of applications including, but not limited to, climate and atmospheric remote sensing studies, trace gas retrievals, and transmission simulations [8]. Organized into several major components, the most recent HITRAN compilation consists of individual line parameters for the resolved molecular transitions spanning the range from the microwave through the infrared and into the visible range, absorption cross-sections for the unresolved molecular transitions in the infrared, line-coupling parameters for CO_2, individual line parameters and cross-sections for molecular transitions in the ultra-violet, and refractive indices of aerosols. Even though the acronym, HITRAN, only came into use with the 1986 line compilation [13], all databases considered in this report were compiled by the same organization. Thus, the HITRAN designation will be used for all line compilations.

Over the last quarter century, significant improvements have been made to the HITRAN compilation of spectroscopic parameters, including those which are most critical to radiative transfer calculations such as line position, line intensity, air-broadened line half-width, and lower state energy. During that time, the size of the HITRAN database increased substantially, to the extent that by the 2004 edition the line parameter portion of the database had swollen to 1,789,569 line transitions representing 39 species. The focus of the present study, however, does not encompass the complete HITRAN database, but rather, is constrained to the thermal infrared (0–3000 cm^{-1}), as well as to the six species representing the original main gas listing: H_2O, CO_2, O_3, N_2O, CO, and CH_4. These trace species account for the climatologically most important molecular line absorption in the thermal infrared, and except for CO, account for the molecular line absorption that is typically included in highly parameterized climate models [19]. Even with this constrained focus, the number of line transitions compiled in the thermal infrared for these six trace species has increased by a factor of 4.5 from 115,200 transitions in the 1982 database to 517,712 transitions in the 2004 database.

Table 1 summarizes the changes that have been made to the thermal infrared portion of the HITRAN database during the 1982–2004 timeframe with respect to the total number of line transitions, total line intensities, average line half-widths, and intensity-weighted line half-widths for the species H_2O, CO_2, O_3, N_2O, CO, and CH_4. Immediately apparent are the substantial increases, for most species, in the total number of line transitions, coupled with only modest changes to the integrated total line intensities. Caution must be exercised, however, when interpreting the total infrared line intensity results, since significant changes in the individual line intensities can easily be lost in the totals. For instance, the modest differences among the total infrared line intensities for CO_2 obscure the significant modifications that had been implemented into the CO_2 line intensities for the 1986 HITRAN database [13] and then again for the 1992 HITRAN database [14,20]. This apparently subtle difference leads to a non-negligible difference in the CO_2 calculations using those editions of the HITRAN database. In addition, for the case of O_3, an earlier study [19] implied that an observed 5% increase in total line intensity for O_3 between the 1986 and 1996 HITRAN databases could be attributed to the large increase in the number of line transitions. The findings of this study demonstrated, however, that imposing a lower line intensity cutoff of 3×10^{-24} to the O_3 line intensities in the 1996 HITRAN database, a criterion that would force the number of lines in that database to be comparable to the number of lines in the 1986 HITRAN database, only reduced the integrated total line intensities by 0.1%. Thus, a modification to the individual line intensities, rather than the total number of line transitions, appears to be the mechanism responsible for increasing the integrated total line intensities [21].

Table 1 also presents average half-width values, which are representative of all the line transitions, and intensity-weighted average half-width values, which characterize the relatively strong, albeit less prevalent, radiatively dominant line transitions responsible for the most significant absorption and emission. Even though a considerable number of additional, mostly weak, line transitions have been incorporated into the HITRAN database over the last 25 years, the changes to the line half-width averages reported in Table 1 are dominated by updates to the individual line half-width values. Note that Table 1 does not include the 33,414 O_3 line transitions in the pure-rotational band for the very rare isotopologues containing ^{17}O that were inadvertently assigned line half-width values of 0.000 cm^{-1} in the 2004 HITRAN database, but which should have been assigned non-zero default values (L. Rothman, private communications). Inclusion of these O_3 line

Table 1
Summary of the line characteristics for the major infrared absorbers listed in the 1982–2004 HITRAN databases from 0 to 3000 cm^{-1}, where N is the total number of spectral lines, ΣS is the sum of line intensities in cm^{-1} (molecule cm^{-2}) where the values $a(b) = a \times 10^b$, $\Sigma\alpha/N$, and $\Sigma S\alpha/\Sigma S$ are the average and line intensity-weighted air-broadened line half-widths in cm^{-1}

HITRAN database	N	ΣS	$\Sigma\alpha/N$	$\Sigma S\alpha/\Sigma S$
Water vapor (H_2O)				
2004	18,429	6.341(−17)	0.06371	0.07882
2000	16,422	6.359(−17)	0.06196	0.07524
1996	15,571	6.347(−17)	0.06259	0.07557
1992	14,650	6.346(−17)	0.06290	0.07557
1986	14,067	6.325(−17)	0.06077	0.07502
1982	15,505	6.326(−17)	0.06030	0.07504
Carbon dioxide (CO_2)				
2004	40,095	1.098(−16)	0.07119	0.07358
2000	38,843	1.098(−16)	0.07120	0.07358
1996	38,843	1.098(−16)	0.07120	0.07358
1992	38,845	1.098(−16)	0.07120	0.07358
1986	38,040	1.141(−16)	0.07118	0.07556
1982	36,253	1.149(−16)	0.06869	0.07194
Ozone (O_3)				
2004	261,878	1.761(−17)	0.07349	0.07640
2000	258,958	1.819(−17)	0.06942	0.07229
1996	258,958	1.819(−17)	0.06942	0.07229
1992	161,525	1.818(−17)	0.06945	0.07229
1986	48,841	1.737(−17)	0.06406	0.06640
1982	42,738	1.789(−17)	0.08589	0.08456
Nitrous oxide (N_2O)				
2004	32,299	6.967(−17)	0.07490	0.07704
2000	20,828	6.974(−17)	0.07443	0.07656
1996	20,827	6.974(−17)	0.07443	0.07656
1992	20,829	6.973(−17)	0.07443	0.07656
1986	20,829	6.973(−17)	0.07443	0.07656
1982	12,549	7.065(−17)	0.07929	0.08263
Carbon monoxide (CO)				
2004	1913	1.012(–17)	0.04935	0.06061
2000	1913	1.012(–17)	0.04794	0.06061
1996	1913	1.012(–17)	0.04794	0.06061
1992	1500	1.052(–17)	0.04894	0.06061
1986	377	9.958(–18)	0.05997	0.06715
1982	377	9.960(–18)	0.05997	0.06715
Methane (CH_4)				
2004	129,684	8.354(−18)	0.04970	0.05858
2000	37,392	8.440(−18)	0.05336	0.05916
1996	37,392	8.440(−18)	0.05336	0.05916
1992	36,775	8.440(−18)	0.05324	0.05916
1986	10,519	8.295(−18)	0.05836	0.05779
1982	7778	8.253(−18)	0.05309	0.05550

All values are for $T = 296$ K and $P = 1013.25$ hPa.

transitions has a negligible impact upon the total infrared line intensity and the intensity-weighted average line half-width for O_3; however, inclusion of these O_3 line transitions does have a profound impact upon the non-weighted average line half-width, decreasing that value from 0.07349 to 0.06518 cm^{-1}. Use of the average half-width value, which includes the default half-width values, can easily lead to a misinterpretation of the results.

While Table 1 highlights the revisions to the HITRAN database that are pertinent to the present study, the published HITRAN reports [8,12–16], and the references therein, provide detailed discussions concerning the

updates for all the spectroscopic parameters that are compiled in the various editions of the HITRAN database.

3. Methods and inputs

Currently, the line-by-line method is the most rigorous approach for theoretically calculating the absorption coefficients that characterize the spectra of molecular species. Thus, this method is ideal for examining the magnitude of the radiative effects resulting from changes to the HITRAN database. The present investigation makes use of the Monochromatic Radiative Transfer Algorithm (MRTA), a line-by-line method originally developed at SUNY Stony Brook in the 1980s to study the radiative effects of infrared-active gases in planetary atmospheres. Over the last decade, MRTA has been used to calculate the radiative forcings attributed to minor trace species [22], to produce correlated k-distribution routines for satellite channels [23], to model the far-infrared at high spectral resolution [24], and to establish the stability of satellite instruments [25]. MRTA has also participated in several line-by-line algorithm inter-comparison studies [4,11], which have clearly demonstrated the ability of this algorithm to agree very favorably with the other participating line-by-line models.

For molecular species with resolvable line structures, the absorption coefficient can be expressed as

$$k_\omega(p,\theta) = \sum_i S_i(\theta) f_{i,\omega}(p,\theta), \tag{1}$$

where ω is the wave number, p is the pressure, θ is the temperature, $S_i(\theta)$ is the intensity of the ith line, and $f_{i,\omega}(p,\theta)$ is the line shape factor. Kratz and Rose [23] have provided a detailed description of the method used in MRTA to calculate the absorption coefficient. To solve Eq. (1) for the absorption coefficients, the line-by-line method relies on the HITRAN compilations [8,12–16] to provide the line locations, intensities, air-broadened half-widths, and lower state energies for the major infrared-active species in the Earth's atmosphere (see Table 1).

For molecular species with unresolved line structures, high-resolution models frequently resort to calculating the absorption coefficients directly from the cross-section data, which are also available from the HITRAN compilations. In the present study, however, the line-by-line method uses a compilation of pseudo-line parameters provided by P. Varanasi (private communications) that can be incorporated into the model to solve Eq. (1) in the same manner as the line parameters used for molecular species with resolved line structures.

Unless otherwise specified, MRTA makes use of the MT_CKD 1.0 continuum formulation [10] to account for the infrared continuum, and neglects the effects of line mixing, which have a relatively small impact upon the total infrared flux, and is generally absent from highly parameterized models. The spectral resolution is taken to be $0.005\,\mathrm{cm}^{-1}$, the zenith and nadir directions are used for radiance calculations, and an 8-point Gaussian quadrature is used for flux calculations.

The temperatures and pressures required to solve Eq. (1) were obtained from the five McClatchey et al. [26] climatological profiles: tropical, mid-latitude summer, mid-latitude winter, sub-arctic summer, and sub-arctic winter. The abundances for H_2O and O_3 were also obtained directly from the McClatchey et al. [26] profiles, while the mixing ratios for the well-mixed species were defined to be 0.78084 ppv for N_2, 0.20948 ppv for O_2, 0.00934 ppv for Ar, 350 ppmv for CO_2, 0.31 ppmv for N_2O, 0.15 ppmv for CO, and 1.75 ppmv for CH_4. In addition, the mixing ratios for the minor trace species were defined to be 0.268 ppbv for CFC-11, 0.503 ppbv for CFC-12, 0.105 ppbv for HCFC-22, 0.132 ppbv for CCl_4, 0.070 ppbv for CF_4, and 0.0025 ppbv for SF_6. The isotopic distribution for each of the species is taken from the HITRAN database (see e.g., Rothman et al. [8], Table 6). The vertical resolutions for all five profiles were defined to be 1 km from the surface at 0 km to an altitude of 25 km, and 5 km from 25 km to the top of atmosphere (TOA) at 70 km. The surface emissivity was taken to be unity, and the calculations were run for clear-sky conditions. Since the calculated results tended to fall within two classes dependent upon the atmospheric profile: warm–moist (tropical and summer atmospheres) and cool–dry (winter atmospheres), for brevity, only the results for the tropical and sub-arctic winter atmospheres are presented.

4. Effects of input changes on the radiative transfer calculations

To address specific effects that can arise from input changes to the line-by-line calculations, the following discussion has been divided into seven subsections. The first four subsections deal directly with the radiative effects resulting from changes to the HITRAN database: the spectral radiances, the broadband fluxes, the radiative forcing due to increases in trace species amounts, and the widely used Fu and Liou model. The fifth subsection briefly highlights the radiative effects associated with changes to the continuum formulations, while the sixth touches upon the impact of CO_2 line mixing whose coefficients were first compiled in the 2004 HITRAN database. The final subsection comments on the reported uncertainties in the HITRAN compilation.

4.1. Spectral radiance calculation results

Spectral radiance calculations have been run for the entire thermal infrared (0–3000 cm^{-1}); however, due to a combination of low radiances and very small differences below 100 cm^{-1} and beyond 1700 cm^{-1}, the spectral radiances are only presented between 100 and 1700 cm^{-1}. Moreover, for clarity, the spectral radiances have been averaged to a resolution of 1.0 cm^{-1}, a resolution that is comparable to the resolutions of the satellite-based Atmospheric Infrared Sounder (AIRS) [27] aboard Aqua, the balloon-borne Far-Infrared Spectroscopy of the Troposphere instrument [28], and the surface-based Atmospheric Emitted Radiance Interferometer (AERI) [29].

4.1.1. Tropical atmosphere

Fig. 1 illustrates the up-welling TOA nadir radiances and Fig. 2 illustrates the down-welling surface zenith radiance as calculated for the tropical atmosphere. The upper plots in Figs. 1 and 2 represent the calculated radiances using the line parameters for H_2O, CO_2, O_3, N_2O, CH_4, and CO from the 2004 HITRAN database, along with the pseudo-line parameters for CFC-11, CFC-12, HCFC-22, CCl_4, CF_4, and SF_6, and the MT_CKD 1.0 continuum. The set of curves in the lower plots of Figs. 1 and 2 represents differences between calculated radiances for successive pairs of HITRAN databases, from top to bottom: HITRAN 2000–HITRAN 2004, HITRAN 1996–HITRAN 2000, HITRAN 1992–HITRAN 1996, HITRAN 1986–HITRAN 1992, and HITRAN 1982–HITRAN 1986. To distinguish among the five comparison sets, results have been vertically offset by 0.014, 0.007, 0.0, −0.007, and −0.014 $W\,m^{-2}\,sr^{-1}(cm^{-1})^{-1}$, respectively. In addition, a $4\times$ scaling factor has been applied to the vertical axis in the lower plot as compared with the upper plot.

The most prominent differences between the calculations using the 1982 and 1986 HITRAN databases for the up-welling TOA radiances illustrated in the lower plot of Fig. 1 are attributable to the extensive updates to both the CO_2 line parameters, affecting the 550–850 cm^{-1} spectral range, and the O_3 line parameters, affecting the 950–1100 cm^{-1} spectral range [13]. To a lesser degree, updates to the H_2O line parameters affect the 150–450 cm^{-1} spectral range in the far-infrared and the 900–1400 cm^{-1} spectral range in the middle infrared, while updates to the N_2O line parameters in the 1100–1200 and 1250–1350 cm^{-1} spectral ranges affect the middle infrared. Because of the substantial opacity due to H_2O in the lower tropical troposphere, differences in the down-welling surface radiances in the lower plot in Fig. 2 are obscured below 700 cm^{-1}, and are diminished greatly for CO_2, O_3, and N_2O but are enhanced noticeably for H_2O between 700 and 1400 cm^{-1}. Integrated over the entire thermal infrared, the TOA radiances calculated using the 1982 HITRAN database are underestimated compared with those calculated using the 1986 HITRAN database; similarly, the surface radiances are overestimated. The significance of these results is further emphasized by examining the prominent difference features located within the remote sensing bands [20,30] at 722.5 and 791.5 cm^{-1}, which, respectively, show TOA radiance differences of −0.0025 and −0.0034 $W\,m^{-2}\,sr^{-1}(cm^{-1})^{-1}$ corresponding to brightness temperature differences of −1.86 and −2.25 K, and surface radiance differences of 0.0010 and 0.0056 $W\,m^{-2}\,sr^{-1}(cm^{-1})^{-1}$ corresponding to brightness temperature differences of 0.62 and 1.67 K. Uncertainties in the brightness temperature retrievals of this magnitude are problematic, especially for optically thick regions of the spectrum where such differences could affect the interpretation of satellite data.

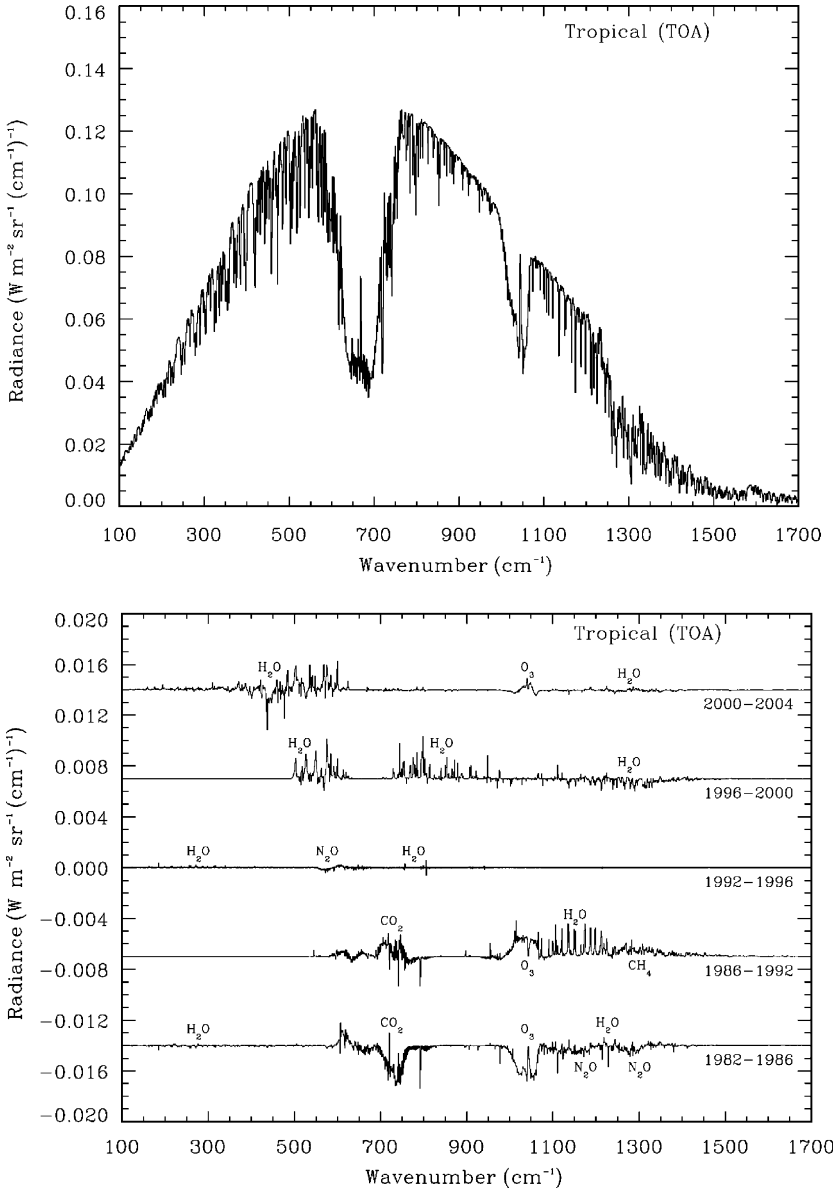

Fig. 1. A comparison of TOA radiance calculations over the spectral range from 100 to 1700 cm^{-1} for the tropical atmosphere. The spectral curve in the upper plot represents the calculated radiances using the line parameters from the HITRAN 2004 database for H_2O, CO_2, O_3, N_2O, CH_4, and CO, along with a static database for the effects of CFC-11, CFC-12, HCFC-22, CCl_4, CF_4, SF_6, and the MT_CKD 1.0 continuum. The curves in the lower plot represent differences between the HITRAN databases: HITRAN 2000–HITRAN $2004+2\delta$, HITRAN 1996–HITRAN $2000+\delta$, HITRAN 1992–HITRAN 1996, HITRAN 1986–HITRAN $1992-\delta$, and HITRAN 1982–HITRAN $1986-2\delta$, where $\delta = 0.007\,W\,m^{-2}\,sr^{-1}(cm^{-1})^{-1}$.

As can be gleaned from the radiance calculations, updates to the HITRAN database from 1982 to 1986 frequently lead to brightness temperature differences exceeding 1 K.

The most prominent differences between the calculations using the 1986 and 1992 HITRAN databases for the up-welling TOA radiances illustrated in the lower plot of Fig. 1 are attributable to the extensive updates to both the CO_2 line parameters, affecting the 550–850 cm^{-1} spectral range, and the O_3 line parameters, affecting the 950–1100 cm^{-1} spectral range [14]. In addition, major updates to the H_2O line parameters have significantly affected the 1050–1500 cm^{-1} spectral range, while updates to the CH_4 line parameters have affected the 1250–1400 cm^{-1} spectral range. The substantial opacity due to H_2O in the lower tropical troposphere

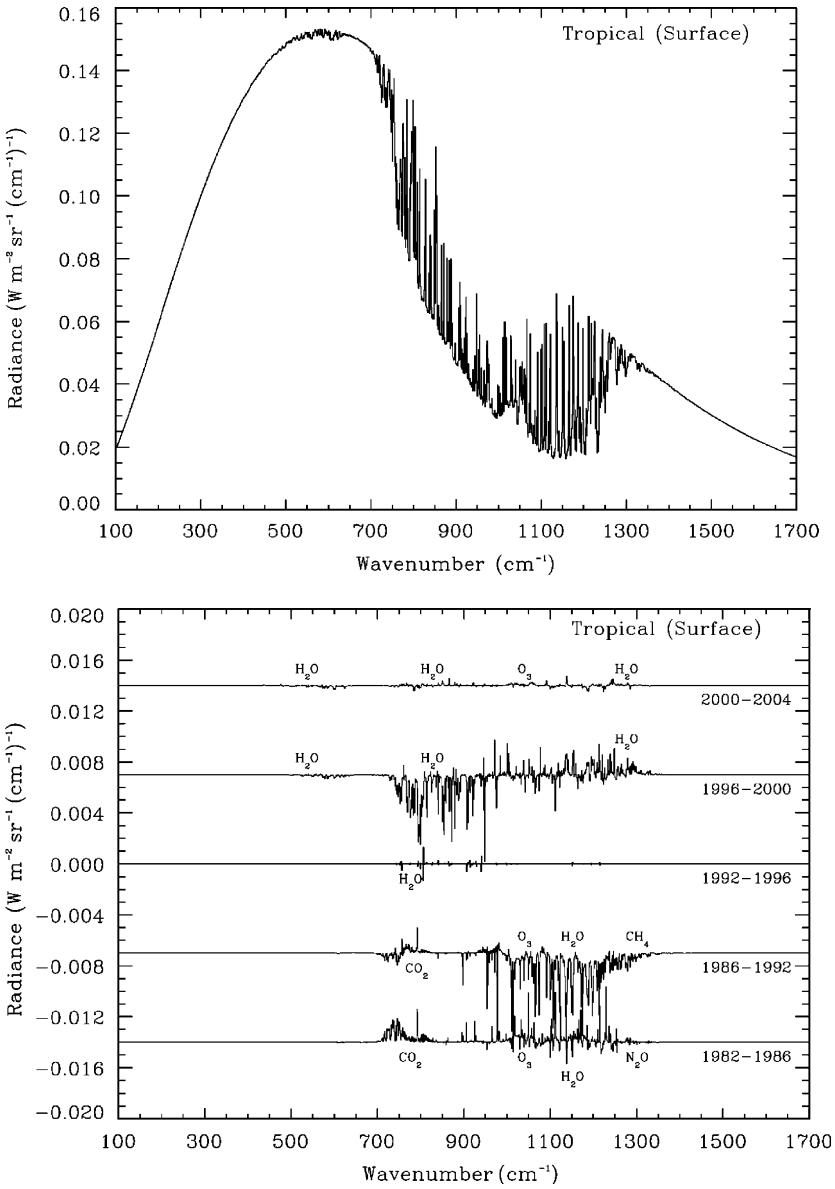

Fig. 2. A comparison of surface radiance calculations analogous to the TOA results presented in Fig. 1.

again causes the differences in the down-welling surface radiances in the lower plot in Fig. 2 to be obscured below 700 cm^{-1}, and to be diminished greatly for CO_2, O_3, and CH_4 but are enhanced noticeably for H_2O between 700 and 1400 cm^{-1}. Integrated over the entire thermal infrared, the TOA radiances calculated using the 1986 HITRAN database are overestimated compared with those calculated using the 1992 HITRAN database; similarly, the surface radiances are underestimated. Re-examining the prominent difference features at 722.5 and 791.5 cm^{-1}, respectively, show TOA radiance differences of 0.0009 and $-0.0023\,W\,m^{-2}sr^{-1}(cm^{-1})^{-1}$ corresponding to brightness temperature differences of 0.78 and -1.52 K, and the surface radiance differences of -0.0005 and $0.0020\,W\,m^{-2}\,sr^{-1}(cm^{-1})^{-1}$ corresponding to brightness temperature differences of -0.32 and 1.33 K. The sign change for the radiance difference for the 722.5 cm^{-1} feature is typical of the compensating differences observed for much of the CO_2 and O_3 bands. In contrast, the results for the 791.5 cm^{-1} feature were additive, further increasing the difference from the 1982 HITRAN

database. Of note are the difference features between 900 and 1250 cm^{-1}, due mostly to H_2O, which are frequently of greater magnitude than the difference features at 722.5 and 791.5 cm^{-1} attributed to CO_2.

The differences between the calculations using the 1992 and 1996 HITRAN databases for the up-welling TOA radiances illustrated in the lower plot in Fig. 1 are quite small. For this case, the updates to the H_2O line parameters only slightly affect the 150–450 cm^{-1} spectral range as well as a few specific wave-number regions in the infrared window region, and updates to the N_2O line parameters only affect the 550–650 cm^{-1} spectral range [15]. The rather modest changes implemented into the 1996 HITRAN database along with the substantial opacity due to H_2O in the lower tropical troposphere have resulted in only a small number of H_2O-induced difference appearing in the down-welling surface radiances in the infrared window region as shown in the lower plot in Fig. 2. The inter-comparison results among the 1986, 1992, and 1996 HITRAN databases shown in Figs. 1 and 2 are consistent with the results shown in Figs. 3 and 4, respectively, of Pinnock and Shine [19] even though their study made use of a global, annual mean atmospheric profile instead of a tropical profile.

The extensive updates to the H_2O line parameters between the 1996 and 2000 HITRAN databases [16] are completely responsible for the differences seen in the up-welling TOA and down-welling surface radiances affecting the 500–1500 cm^{-1} spectral range illustrated in the lower plots in Figs. 1 and 2. Although the differences are confined to just H_2O, they are substantial, as can be appreciated by examining the prominent difference at 948.5 cm^{-1}. In this case, the TOA and surface radiance differences are 0.0018 and $-0.0068\,W\,m^{-2}\,sr^{-1}(cm^{-1})^{-1}$, respectively, 2% and 10% of the spectral radiance at that wave-number location, and correspond to brightness temperature differences of 1.19 and −5.53 K.

Differences between the calculations using the 2000 and 2004 HITRAN databases for the up-welling TOA radiances in the lower plot of Fig. 1 are mostly attributable to major improvements in the H_2O line parameters across the entire thermal infrared but chiefly affect the 100–700 and 1100–1400 cm^{-1} spectral ranges. In addition, major improvements in the O_3 line parameters also affect the 1000–1100 cm^{-1} spectral range [8]. The most notable differences associated with improvements to the H_2O line parameters are in the far-infrared (100–650 cm^{-1}), which further the improvements made to the H_2O line parameter in the HITRAN 2000 database for this spectral range which holds great promise for improving our understanding of the Earth's climate [31,32]. As previously noted, however, the substantial opacity attributed to H_2O in the lower tropical troposphere obscures the differences in the down-welling surface radiances below 700 cm^{-1}.

4.1.2. Sub-arctic winter atmosphere

While warm, moist atmospheric conditions are opaque to far-infrared radiation, cold, dry atmospheric conditions tend to be noticeably less affected by water vapor absorption [29]. Thus, re-examining the difference calculations using the cool, dry conditions in the sub-arctic winter can provide an alternate perspective [4] of the effects caused by changes in the HITRAN compilations. As anticipated [4], the differences in the up-welling TOA radiance calculations for the sub-arctic winter atmosphere, as shown in Fig. 3, are fairly similar to, albeit noticeably smaller than, those encountered for the tropical atmosphere in Fig. 1. At this stage, there appears to be merit to the conclusion drawn by Pinnock and Shine [19] that "the sub-arctic winter atmosphere is the least sensitive to the HITRAN changes simply because the irradiances are smaller in the spectral regions, such as in the water vapor window where the changes have the largest effect." The comparison of the down-welling surface radiances in Fig. 4 for the sub-arctic winter atmosphere to those in Fig. 2 for the tropical atmosphere, however, dramatically demonstrates that the sub-arctic winter atmosphere can, at times, actually be more sensitive to the changes in the HITRAN line parameters than the tropical atmosphere. This is most evident when comparing the radiance differences attributed to changes in the H_2O line parameters within the 400–600 cm^{-1} spectral range. Indeed, the radiance differences shown in Fig. 4 between the 2000 and 2004 HITRAN databases, and between the 1996 and 2000 HITRAN databases for the sub-arctic winter atmosphere are among the most prominent in this study. In contrast, the down-welling surface radiance differences shown in Fig. 2 for the tropical atmosphere reveal virtually no sensitivity to the changes in the H_2O line parameters in the far-infrared. In addition, the comparison between Figs. 4 and 2 also reveals that the radiative effects of changes to the CO_2 line parameters between 550 and 850 cm^{-1} and to the O_3 line parameters between 950 and 1100 cm^{-1} are much more distinct in Fig. 4.

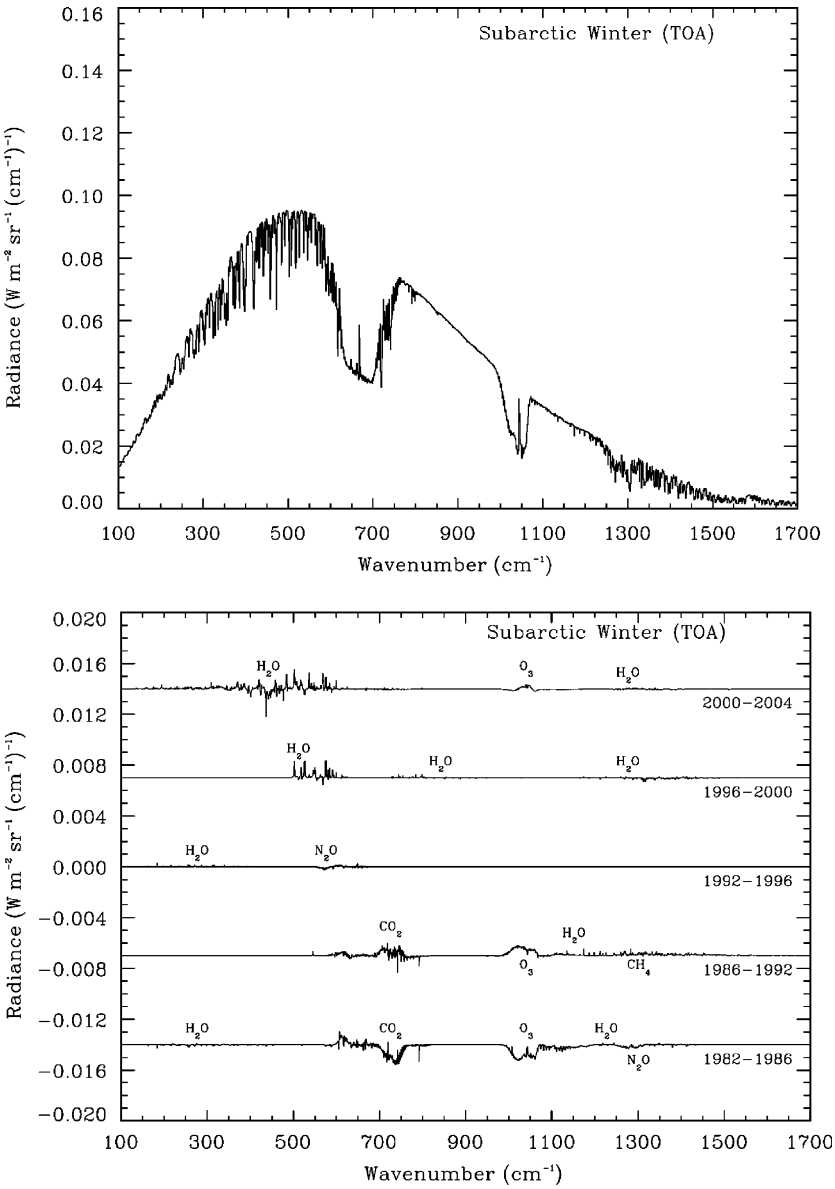

Fig. 3. A comparison of TOA radiance calculations for the sub-arctic winter atmosphere analogous to the results presented in Fig. 1 for the tropical atmosphere.

The difference between the sensitivity of the tropical (Figs. 1 and 2) and sub-arctic winter atmospheres (Figs. 3 and 4) to the changes in the H_2O line parameters between the 2000 and 2004 HITRAN can be further appreciated by examining the prominent difference at 437.5 cm^{-1}. In this case, the TOA and surface radiance differences using the tropical atmosphere are −0.0015 and 0.0001 $W\,m^{-2}\,sr^{-1}(cm^{-1})^{-1}$, respectively, 1.4% and 0.05% of the spectral radiance, which correspond to brightness temperature differences of −1.48 and 0.06 K. However, the TOA and surface radiance differences using the sub-arctic winter atmosphere are −0.0005 and 0.0048 $W\,m^{-2}\,sr^{-1}(cm^{-1})^{-1}$, respectively, 0.5% and 6.4% of the spectral radiance, and correspond to brightness temperature differences of −0.47 and 5.27 K. Thus, the higher H_2O amounts and temperature difference between the surface and TOA in the tropical atmosphere produce a larger TOA signal; however, the higher H_2O amounts also obscure any signal at the surface. In contrast, the lower H_2O amounts in the sub-arctic winter atmosphere produce a larger signal at the surface but also produce a smaller TOA signal. Thus, the conclusion drawn by

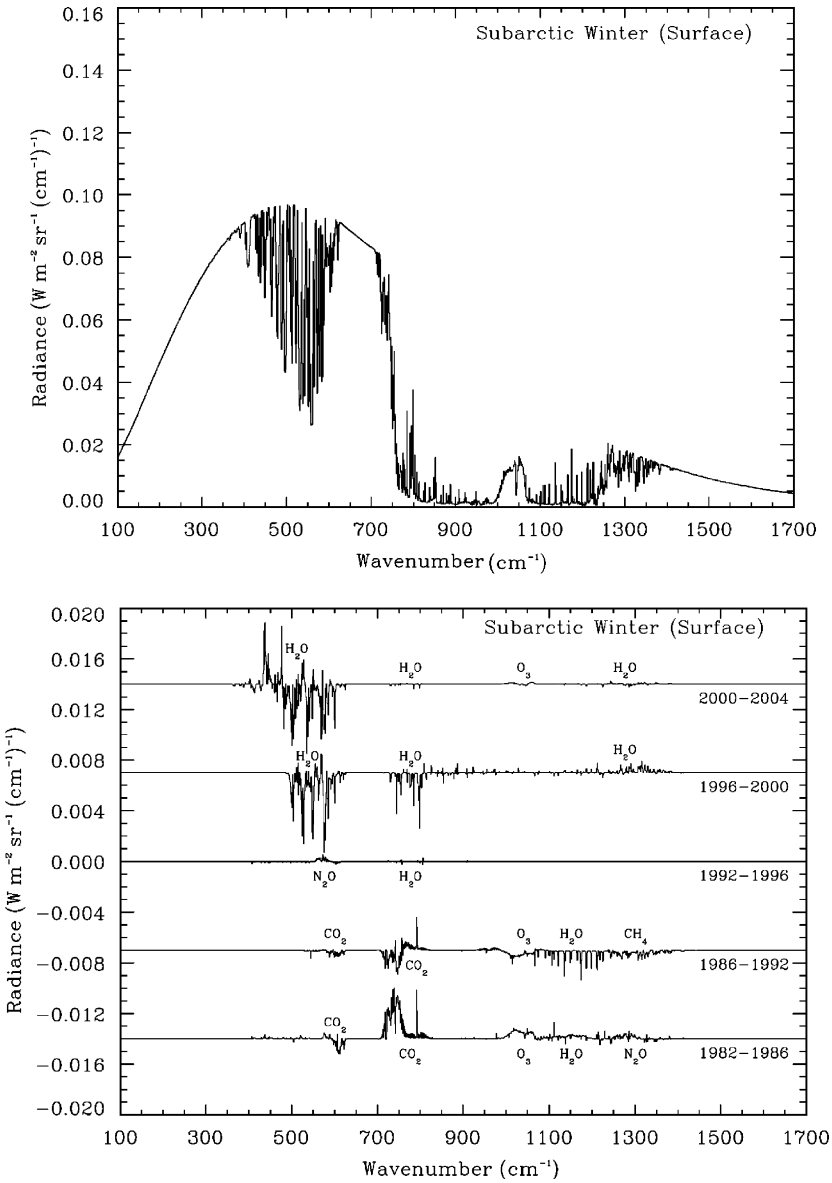

Fig. 4. A comparison of surface radiance calculations for the sub-arctic winter atmosphere analogous to the results presented in Fig. 3 for the tropical atmosphere.

Pinnock and Shine concerning the sub-arctic winter atmosphere is misleading since the sub-arctic winter atmosphere is not always the least sensitive to changes in the HITRAN database, especially with regard to downwelling radiances in the far-infrared, and the H_2O amount appears to be of comparable importance to the magnitude of the thermal emitted energy in revealing the effects of changes to the HITRAN database. Moreover, many of the radiance differences resulting from the difference line parameters in the various HITRAN databases are located outside of the infrared window region (830–1250 cm^{-1}).

4.2. Integrated flux calculation results

While spectral radiance calculations provide a measure of the degree to which changes in the line parameters can affect the interpretation of satellite retrievals, flux calculations emphasize the impact that changes to the

Table 2
Comparison of fluxes ($W\,m^{-2}$) calculated for the spectral range from 0 to $3000\,cm^{-1}$

HITRAN database	F_{up} (TOA)	F_{net} (Tropopause)	F_{dn} (Surface)
Tropical (TRO)			
2004	287.366	276.224	394.560
2000–2004	0.214	0.227	−0.057
1996–2004	0.439	0.456	−0.389
1992–2004	0.447	0.473	−0.390
1986–2004	1.369	1.309	−1.475
1982–2004	0.279	0.511	−1.071
Sub-arctic winter (SAW)			
2004	198.016	171.071	174.619
2000–2004	0.091	0.262	−0.260
1996–2004	0.149	0.331	−0.713
1992–2004	0.151	0.359	−0.706
1986–2004	0.425	0.681	−1.026
1982–2004	−0.062	0.190	−0.493

Calculations include the line parameters of H_2O, CO_2, O_3, N_2O, CO, and CH_4 from the designated HITRAN database as well as a static database for the effects of CFC-11, CFC-12, HCFC-22, CCl_4, CF_4, SF_6, and the MT_CKD 1.0 continuum.

HITRAN database have on climate calculations. Table 2 presents line-by-line calculations for the up-welling TOA fluxes (F_{up}), net tropopause fluxes (F_{net}), and down-welling surface fluxes (F_{dn}) covering the entire thermal infrared (0–$3000\,cm^{-1}$) for the tropical and sub-arctic winter atmospheres. The tropopause altitude has been taken to be 17 km for the tropical atmosphere, and 9 km for the sub-arctic winter atmosphere. To elucidate the effects of the changes in the line parameter compilations, fluxes calculated using the 2004 HITRAN database are presented along with the flux differences between the older HITRAN databases and the 2004 HITRAN database. Among the four most recent line compilations, there appears to be a fairly systematic convergence toward the results using the 2004 HITRAN database with flux differences being of order 0.1–$0.5\,W\,m^{-2}$ for the tropical atmosphere and 0.1–$0.7\,W\,m^{-2}$ for the sub-arctic winter atmosphere. Calculations using the 1986 HITRAN database, however, compare less favorably, yielding flux differences of order 1.3–$1.5\,W\,m^{-2}$ for the tropical atmosphere and 0.4–$1.0\,W\,m^{-2}$ for the sub-arctic winter atmosphere. In contrast, the use of the 1982 database appears to be an improvement upon the 1986 HITRAN database, producing flux differences of order 0.3–$1.1\,W\,m^{-2}$ for the tropical atmosphere and 0.1–$0.5\,W\,m^{-2}$ for the sub-arctic winter atmosphere. As will be demonstrated, however, dividing the thermal infrared into subintervals reveals this to be a serendipitous cancellation of errors.

To gain a better understanding of the results shown in Table 2, flux calculations were also run for several intervals subdividing the thermal infrared. The results for two of the subintervals, the far-infrared (100–$650\,cm^{-1}$) and the Clouds and the Earth's Radiant Energy System (CERES) window channel [25,33] (848–$1235\,cm^{-1}$), are, respectively, shown in Tables 3 and 4 using the same format as used for Table 2. As anticipated from Figs. 1–4, the results in Table 3 pertaining to the four oldest line compilations demonstrate little sensitivity to changes in the line parameters in the far-infrared, while the flux differences associated with the use of the 2000 HITRAN database are intermediate between the older databases and the 2004 HITRAN database. In addition, nearly all of the broadband thermal infrared flux differences shown in Table 2 between the 2004 HITRAN database and the three previous databases (1992, 1996, and 2000) occur in the far-infrared, with one notable exception, the down-welling flux at the surface in the tropical atmosphere. As previously noted, the extreme H_2O opacity of the far-infrared portion of the tropical atmosphere obscures nearly any difference caused by changes in the line parameters. As anticipated from the results in Tables 2 and 3, the results in Table 4 show little sensitivity among the four most recent line compilations with the exception of the down-welling flux in the tropical atmosphere where nearly 45% of the broadband thermal infrared flux differences between the 1992 and 2004 HITRAN databases are taken into account inside the infrared window region. In contrast, the flux differences in the infrared window region between the two oldest line compilations and the 1992 HITRAN database account for a significant fraction of the flux differences between the two oldest line compilations and the 2004 HITRAN database for the entire thermal infrared.

Table 3
Comparison of fluxes ($W\,m^{-2}$) calculated for the spectral range from 100 to 650 cm^{-1}

HITRAN database	F_{up} (TOA)	F_{net} (Tropopause)	F_{dn} (Surface)
Tropical (TRO)			
2004	120.120	114.256	189.315
2000–2004	0.189	0.248	−0.015
1996–2004	0.369	0.432	−0.038
1992–2004	0.377	0.451	−0.039
1986–2004	0.409	0.464	−0.039
1982–2004	0.436	0.507	−0.039
Sub-arctic winter (SAW)			
2004	105.234	86.907	119.801
2000–2004	0.105	0.286	−0.282
1996–2004	0.179	0.371	−0.638
1992–2004	0.182	0.401	−0.631
1986–2004	0.199	0.427	−0.657
1982–2004	0.217	0.454	−0.668

Table 4
Comparison of fluxes ($W\,m^{-2}$) calculated for the spectral range from 848 to 1235 cm^{-1} (CERES Window)

HITRAN database	F_{up} (TOA)	F_{net} (Tropopause)	F_{dn} (Surface)
Tropical (TRO)			
2004	92.850	95.702	62.137
2000–2004	−0.008	−0.055	−0.029
1996–2004	0.043	−0.005	−0.173
1992–2004	0.043	−0.004	−0.175
1986–2004	0.618	0.478	−1.131
1982–2004	−0.009	0.132	−0.875
Sub-arctic winter (SAW)			
2004	44.759	46.230	6.407
2000–2004	−0.010	−0.022	0.020
1996–2004	−0.011	−0.023	0.011
1992–2004	−0.011	−0.023	0.011
1986–2004	0.136	0.089	−0.201
1982–2004	−0.155	−0.096	−0.002

Calculations include the line parameters of H_2O, CO_2, O_3, N_2O, CO, and CH_4 from the designated HITRAN database as well as a static database for the effects of CFC-11, CFC-12, HCFC-22, CCl_4, CF_4, SF_6, and the MT_CKD 1.0 continuum.

Table 5 provides a synopsis of the relative contributions of the microwave (0–100 cm^{-1}), far-infrared (100–650 cm^{-1}), 15 μm CO_2 (650–848 cm^{-1}), CERES infrared window (848–1235 cm^{-1}), and middle-infrared (1235–3000 cm^{-1}) bands as compared with the total thermal infrared (0–3000 cm^{-1}) for the flux differences between the 1982 and 2004 HITRAN databases. The extremely large fractional contributions, frequently exceeding 1.0, demonstrate that the apparently reasonable agreement in Table 2 between the 1982 and 2004 HITRAN databases, especially for the up-welling fluxes, is an artifact produced by the cancellation of significant differences. Comparisons between the other line compilations and the 2004 HITRAN database do not show such large compensations, and thus, flux differences for those cases in Table 2 are fairly accurate representations of the differences among those databases.

4.3. Radiative forcing: doubling of CO_2, N_2O, and CH_4

The most significant and best understood anthropogenic forcing of the Earth's climate has been attributed to radiative effects caused by increases in the concentrations of the infrared-active trace species CO_2, N_2O,

Table 5
Fractional change $[(F_{1982}(\Delta\omega)-F_{2004}(\Delta\omega))/(F_{1982}(\mathrm{TIR})-F_{2004}(\mathrm{TIR}))]$ of the calculated fluxes associated with the spectral intervals within the infrared versus the total infrared (TIR = 0–3000 cm^{-1}) and attributed to the substitution of the 1982 HITRAN database for the 2004 HITRAN database

$\Delta\omega$ (cm^{-1})	R_{up} (TOA)	R_{net} (Tropopause)	R_{dn} (Surface)
Tropical (TRO)			
0–100	0.0065	0.0041	0.0000
100–650	1.5630	0.9933	0.0369
650–848	−0.7420	−0.3764	0.1384
848–1235	−0.0327	0.2584	0.8171
1235–3000	0.2052	0.1206	0.0076
Sub-arctic winter (SAW)			
0–100	−0.0178	0.0326	0.0000
100–650	−3.5105	2.3884	1.3578
650–848	2.4637	−1.1147	−0.3785
848–1235	2.5073	−0.5042	0.0026
1235–3000	−0.4427	0.1979	0.0181

Calculations include the line parameters for H_2O, CO_2, O_3, N_2O, CO, and CH_4, as well as a static database for the effects of CFC-11, CFC-12, HCFC-22, CCl_4, CF_4, SF_6, and the MT_CKD 1.0 continuum.

CH_4, CFC-11, and CFC-12 [11]. To assess the accuracy of model simulations of past, present, and future climate conditions, Collins et al. [11] formulated a study to inter-compare the radiative forcing computations from benchmark line-by-line methods and parameterized algorithms used in coupled atmosphere–ocean general circulation models. Although this inter-comparison study found excellent agreement among the benchmark line-by-line calculations, there were significant discrepancies among the parameterized model results, as well as between the line-by-line calculations and the parameterized model results. While some of the discrepancies could be explained, Collins et al. [11] concluded that imprecise simulations of the radiative effects attributed to increases in the infrared-active trace species would have "significant implications for the interpretation of climate change simulations." Thus, to estimate the potential contribution that changes in the HITRAN compilation have in causing these discrepancies, line-by-line calculations were run to determine the thermal infrared radiative forcing due to the simultaneous doubling of the mixing ratios of CO_2 (350–700 ppmv), N_2O (0.31–0.62 ppmv), and CH_4 (1.75–3.50 ppmv). This study has adopted the Collins et al. [11] definition for radiative forcing: an instantaneous change in fluxes without stratospheric adjustment. Thus, the present results are directly comparable to the results in the Collins et al. report [11], but not to the results in the IPCC 2007 report [1].

The results, summarized in Table 6, clearly show that the differences in the radiative forcing calculations using the various HITRAN databases are small fractions of the total radiative forcing. Indeed, changes to the HITRAN database induce noticeably smaller differences among the radiative forcing calculations in Table 6 than among the radiative flux differences in Table 2, especially among the four most recent HITRAN databases where the radiative forcing differences are frequently much less than 0.1 $\mathrm{W\,m^{-2}}$. Even the largest overall radiative forcing difference, 0.252 $\mathrm{W\,m^{-2}}$ between the 1982 and 2004 HITRAN databases for the net forcing at the tropopause in the tropical atmosphere, cannot explain the range in radiative forcing projections computed using highly parameterized models [1]. Additional calculations involving the doubling of CO_2, N_2O, and CH_4, separately, as well as calculations simulating the precise conditions considered by Collins et al. [11] have produced similar conclusions. Indeed, for case 2b-1a of Collins et al. [11], a doubling of the CO_2 mixing ratio from 287 to 574 ppmv, even the largest radiative forcing difference, 0.131 $\mathrm{W\,m^{-2}}$, is quite small when compared with the reported spread of parameterized model results in their Fig. 4 [11]. Thus, the differences in the line parameters from the HITRAN database are not the source of the significant discrepancies in the parameterized model radiative forcing calculations, a conclusion consistent with the Forster et al. [1] assessment.

Table 6
Comparison of radiative forcings ($W\,m^{-2}$) calculated for a doubling of CO_2, CH_4, and N_2O for the spectral range from 0 to 3000 cm^{-1}

HITRAN database	F_{up} (TOA)	F_{net} (Tropopause)	F_{dn} (Surface)
Tropical (TRO)			
2004	−4.762	−7.360	1.839
2000–2004	−0.019	−0.019	0.001
1996–2004	−0.034	−0.034	0.015
1992–2004	−0.043	−0.045	0.015
1986–2004	−0.139	−0.130	0.124
1982–2004	−0.230	−0.252	0.152
Sub-arctic winter (SAW)			
2004	−2.391	−4.496	3.230
2000–2004	−0.006	−0.008	0.035
1996–2004	−0.010	−0.012	0.081
1992–2004	−0.017	–0.022	0.091
1986–2004	–0.036	–0.040	0.207
1982–2004	–0.080	–0.095	0.236

Calculations include the line parameters of H_2O, CO_2, O_3, N_2O, CO, and CH_4 from the designated HITRAN database as well as a static database for the effects of CFC-11, CFC-12, HCFC-22, CCl_4, CF_4, SF_6, and the MT_CKD 1.0 continuum.

4.4. Calculations for the Fu and Liou infrared spectral intervals

The Fu and Liou [18] radiative transfer model has proven to be a valuable tool for studies ranging from the theoretical investigation of cirrus clouds [7] to the derivation of surface and atmospheric radiation budget values from satellite-measured radiances [34]. At the core of the Fu and Liou [18] model is an algorithm based on correlated *k*-distribution coefficients that were derived using the 1982 version of the HITRAN database. Considering the significant improvements in the line parameter compilations since the release of the 1982 HITRAN database, and the observed discrepancies between the results of the 1982 database and the most recent line parameter compilation (see Figs. 1–4, Tables 2–5), there is concern that the correlated *k*-distribution coefficients may need to be re-derived. Table 7 shows the percentage differences derived for each of the 12 thermal infrared bands considered by Fu and Liou [18]. Unlike Table 5, which examines the fractional contribution of each interval to the total difference, Table 7 merely provides the percentage differences encountered in each interval when using the 1982 line parameters rather than the 2004 line parameters. The largest difference, −2.5%, occurs at the surface in the tropical atmosphere for the 1100–1250 cm^{-1} interval, and corresponds to a difference of $-0.47\,W\,m^{-2}$ in the down-welling surface flux. This discrepancy exceeds the 1% accuracy achievable with correlated *k*-distribution models [35], and thus implies that revision with the most recent line parameters may be warranted. Nevertheless, when taken in combination with the other thermal infrared intervals used in the Fu and Liou model, the difference between the 1982 and 2004 HITRAN databases has been found to be less than 1% (see e.g., Table 2). Thus, for calculations requiring thermal infrared fluxes with accuracies of order $1\,W\,m^{-2}$, the use of the 1982 HITRAN database in the creation of the correlated *k*-distribution coefficients should not be the driving force behind an initiative to upgrade the Fu and Liou model.

4.5. Effects of changes to the continuum formulations

Although the HITRAN database does not currently compile spectroscopic parameters for the infrared and visible continuum, which has been attributed to non-Lorentzian far wing line shapes [5], radiative transfer models must accurately account for the substantial opacity attributed to the continuum. To satisfy this need, Atmospheric and Environmental Research provides a continuum code as part of their collection of radiative transfer models and databases [10]. Analogous to the HITRAN line parameter compilations, as new

Table 7
Percentage change $[100(F_{1982}(\Delta\omega)/F_{2004}(\Delta\omega)-1.0)]$ in the calculated fluxes for the infrared spectral intervals (given in cm^{-1}) associated with the Fu and Liou [18] model and attributed to the substitution of the 1982 HITRAN database for the 2004 HITRAN database

$\Delta\omega$ (cm^{-1})	R_{up} (TOA)	R_{net} (Tropopause)	R_{dn} (Surface)
Tropical (TRO)			
0–280	0.155	0.405	0.000
280–400	0.142	0.191	0.000
400–540	0.224	0.235	−0.005
540–670	0.852	1.071	−0.058
670–800	−0.618	−0.716	−0.162
800–980	0.090	0.091	−0.737
980–1110	−0.588	−0.185	−0.875
1100–1250	0.314	0.480	−2.513
1250–1400	0.125	0.153	−0.101
1400–1700	0.957	1.018	−0.006
1700–1900	0.423	0.433	−0.005
1900–2200	0.007	0.004	0.205
Sub-arctic winter (SAW)			
0–280	0.099	1.405	0.001
280–400	0.129	0.377	−0.001
400–540	0.155	0.205	−0.680
540–670	0.410	0.828	−1.252
670–800	−0.640	−1.209	0.711
800–980	−0.046	−0.044	1.319
980–1100	−0.860	−0.530	1.223
1100–1250	−0.450	−0.196	−2.485
1250–1400	−0.041	0.014	−0.061
1400–1700	0.853	1.156	0.008
1700–1900	0.369	0.427	−0.043
1900–2200	1.096	−0.045	−0.311

Calculations include the line parameters for H_2O, CO_2, O_3, N_2O, CO, and CH_4, as well as a static database for the effects of CFC-11, CFC-12, HCFC-22, CCl_4, CF_4, SF_6, and the MT_CKD 1.0 continuum.

spectroscopic measurements have become available, the algorithms and requisite datasets describing the continuum have undergone significant modifications [10]. The importance of the updates to the continuum formulations is apparent from a recent far-infrared inter-comparison study [4], which reported that the most energetically significant differences among the participating line-by-line models could be attributed to the choice of continuum code.

Table 8 summarizes the total thermal infrared fluxes that were calculated using the MT_CKD 1.0 continuum code [10], which has been used for most of the calculations in this study, along with the differences between that set of fluxes and the fluxes calculated using the recently released MT_CKD 1.2 continuum code, two CKD continuum codes [5], and the classic RSB continuum algorithm [36]. With the exception of the RSB continuum code, the differences among the various continuum codes are comparable to the differences shown in Table 2 for the differences among the flux calculations using the various HITRAN databases. The larger discrepancies in the calculations based on the RSB continuum can be attributed to that algorithm's use of a very simple formula that calculates only the water vapor continuum absorption in the infrared window region. In contrast, the MT_CKD and CKD continua are calculated using highly sophisticated, physically consistent algorithms that take into consideration the continuum absorption features of water vapor, carbon dioxide, ozone, oxygen, and nitrogen. Additional calculations, not presented here, have demonstrated that nearly all of the differences between MT_CKD 1.0 and 1.2 continuum results are in the far-infrared, while the differences between MT_CKD 1.0 and the other continuum codes occur both in the far-infrared and in the mid-infrared. For further information concerning the continuum formulations, the reader is directed to Clough et al. [10] and the references therein.

Table 8
Comparison of fluxes ($W\,m^{-2}$) calculated for the spectral range from 0 to 3000 cm^{-1} used to examine the effects of changes to the continuum code

Continuum formulation	F_{up} (TOA)	F_{net} (Tropopause)	F_{dn} (Surface)
Tropical (TRO)			
MT_CKD1.0	287.366	276.224	394.560
MT_CKD1.2–MT_CKD1.0	0.214	0.181	−0.005
CKD2.4–MT_CKD1.0	0.690	0.723	−0.550
CKD2.1–MT_CKD1.0	−0.484	−0.394	−0.500
RSB–MT_CKD1.0	2.780	2.920	1.096
Sub-arctic winter (SAW)			
MT_CKD1.0	198.016	171.071	174.619
MT_CKD1.2–MT_CKD1.0	0.169	0.112	−0.344
CKD2.4–MT_CKD1.0	0.295	0.206	−0.954
CKD2.1–MT_CKD1.0	−0.688	−1.195	−0.116
RSB–MT_CKD1.0	1.642	2.926	−2.716

Calculations include the line parameters of H_2O, CO_2, O_3, N_2O, CO, and CH_4 from the 2004 HITRAN database as well as a static database for the effects of CFC-11, CFC-12, HCFC-22, CCl_4, CF_4, SF_6, and the designated continuum.

Table 9
Comparison of fluxes ($W\,m^{-2}$) calculated for the spectral range from 0 to 3000 cm^{-1} used to examine the effects of first-order CO_2 line mixing according to (1) Strow et al. [40] and (2) Rodrigues et al. [37]

Line mixing formulation	F_{up} (TOA)	F_{net} (Tropopause)	F_{dn} (Surface)
Tropical (TRO)			
	287.366	276.224	394.560
CO_2 line mixing (1)	287.699	276.338	394.532
CO_2 line mixing (2)	287.694	276.329	394.528
Sub-arctic winter (SAW)			
	198.016	171.071	174.619
CO_2 line mixing (1)	198.147	171.231	174.516
CO_2 line mixing (2)	198.141	171.222	174.522

Calculations include the line parameters of H_2O, CO_2, O_3, N_2O, CO, and CH_4 from the 2004 HITRAN database as well as a static database for the effects of CFC-11, CFC-12, HCFC-22, CCl_4, CF_4, SF_6, and the MT_CKD1.0 continuum.

4.6. Effects of first order CO_2 line mixing

The 2004 HITRAN database is the first HITRAN compilation to provide line-mixing data for the Q-branches of CO_2 [8]. In addition to the downloadable directories of subroutines and data files, which are based on the research by Hartmann and collaborators [37,38], the 2004 HITRAN database also includes a detailed guide for implementing the line-mixing data into line-by-line codes. The two most prominent CO_2 line-mixing features in the thermal infrared appear at 618 and 721 cm^{-1}. Calculations have shown that neglecting CO_2 line mixing can significantly affect the up-welling and down-welling radiances [4], and, as a consequence, can significantly affect remote sensing retrievals, especially at high resolution. Indeed, neglecting CO_2 line mixing can cause brightness temperature discrepancies of order 5–10 K at a resolution of 0.005 cm^{-1}, and can even produce a 1 K underestimation of the TOA brightness temperature retrieval for band 35 (710.0–725.5 cm^{-1}) of the satellite-based Moderate Resolution Imaging Spectrometer (MODIS) [39] on Aqua and Terra. Integrating over the entire thermal infrared (see Table 9), however, reveals that neglecting CO_2 line mixing induces only a modest effect on the fluxes for both the tropical atmosphere: $F_{up}(\text{TOA}) = -0.33\,W\,m^{-2}$, $F_{dn}(\text{Surface}) = +0.03\,W\,m^{-2}$, and the sub-arctic winter atmosphere: $F_{up}(\text{TOA}) = -0.13\,W\,m^{-2}$, $F_{dn}(\text{Surface}) = +0.10\,W\,m^{-2}$. An inter-comparison of the first-order CO_2 line-mixing approaches of Strow et al. [40] and Rodrigues et al. [37]

Table 10
Estimates of the average percent uncertainty for line intensity (S), air-broadened half-width (γ_{air}), and temperature-dependence of half-width (n_{air}) for the total number (N) of thermal infrared (0–3000 cm^{-1}) spectral lines in the 2004 HITRAN compilation

Species	N	S	γ_{air}	n_{air}
H_2O	18,429	10–20	5–10	10–20
CO_2	40,095	5–10	5–10	5–10
O_3	261,878		10–20	10–20
N_2O	32,299	2–5	2–5	5–10
CO	1913	1–2	2–5	10–20
CH_4	129,684	10–20		$\geqslant 20$

Blank fields indicate a high percentage of unreported, unavailable, or estimated uncertainty ranges.

reveals very small flux differences, which are less than 0.01 $W\,m^{-2}$ for both the tropical and sub-arctic winter atmospheres. Despite this small flux difference, these first-order approaches still have the capability of producing significant brightness temperature differences of order 1 K.

4.7. Uncertainties in the HITRAN line parameters

Pinnock and Shine [19] have presented a fairly thorough analysis of the radiative effects associated with the uncertainties in the line parameters. In their study, the authors considered both correlated uncertainties that result in systematic offsets, and uncorrelated uncertainties that result in random effects. Given reasonable estimates of the uncertainties, which they took to be 5% for the line intensity and 10% for the line half-width, the authors postulated that the errors in the line parameters should be bound between their systematic and random extremes. The results for the sum of line intensities and the average line half-widths presented in Table 1 support their hypothesis as being reasonable.

Uncertainty indices have been reported on the HITRAN database for the line positions (ω), intensities (S), and air-broadened half-widths (γ_{air}) since 1986, and for the self-broadened half-widths (γ_{self}), the temperature dependences of the half-widths (n_{air}), and the pressure-induced line shifts (δ_{air}) since 2000. Average values are summarized in Table 10 for several of the uncertainty indices reported in the 2004 HITRAN compilation [8]. These results suggest that the random errors for the line intensities may be somewhat larger than 5% for several of the major infrared-active species. Even if the uncertainties are constrained to neglect line transitions that have line intensity uncertainties classified as unreported, unavailable, or estimated (see Table 5, Rothman et al.[8]), the average uncertainty index for the line intensities correspond to uncertainties in the 5–10% range for H_2O, CO_2, and O_3, and in the 10–20% range for CH_4. Since no reasonable criteria are available to determine the degree to which the uncertainties are correlated, the present study remained focused solely upon the differences among the reported HITRAN databases.

5. Conclusions

The present study has determined that changes to the spectroscopic parameters, such as the line parameters in the HITRAN database, the continuum formulation, and the CO_2 line-mixing formulation, can profoundly influence the interpretation of high spectral resolution radiance measurements such as those taken by AIRS aboard the Aqua satellite, and AERI from the Earth's surface. Even retrievals from moderate-resolution instruments such as MODIS aboard the Aqua and Terra satellites can be noticeably affected, especially for the optically thick cloud-top altitude bands, such as those around 750 cm^{-1}. In contrast, changes to the HITRAN database only modestly affect broadband retrievals of integrated radiances, such as those taken by CERES aboard the Aqua and Terra satellites. Indeed, the differences among the four most recent line compilations for the simulated CERES window channel TOA radiances and fluxes tended to be significantly better than 0.1%.

The substantial changes to the HITRAN line parameters from 1982 to 1992, most notably CO_2 in the 550–850 cm^{-1} range, O_3 in the 950–1100 cm^{-1} range, and H_2O in the 900–1500 cm^{-1} region, have induced only modest differences, of order 1 $W\,m^{-2}$, in the calculation of the total thermal infrared flux. This apparently

good agreement, however, is an artifact of a cancellation of much larger differences for the subintervals constituting the thermal infrared. Indeed, for calculations comparing the 1982 and 2004 HITRAN databases, the fractional differences for the spectral subintervals can be several times greater than the fractional difference for the entire thermal infrared. In contrast, among the four most recent HITRAN databases there appears to be a fairly systematic convergence toward the results based on the 2004 HITRAN database.

The present study has also found that the cool, dry sub-arctic winter atmosphere can be as sensitive to changes in the HITRAN database as the warm, moist tropical atmosphere. This result, which is contrary to a conclusion from an earlier study, has been attributed not only to the sub-arctic winter atmosphere having noticeably less opacity than the tropical atmosphere, especially in the 400–600 cm^{-1} range, but also to the H_2O line parameters in the far-infrared having been significantly updated since the earlier study was published. Indeed, calculations have shown that nearly all of the broadband thermal infrared differences among the four most recent HITRAN databases can be ascribed to changes in the H_2O line parameters in the far-infrared. The notable exception is the down-welling flux at the surface for the tropical atmosphere where the differences are equally divided between the line parameter changes in the infrared window and middle infrared (1235–3000 cm^{-1}). The magnitude of the changes attributed to the previously unrealized discrepancies in the far-infrared H_2O line parameters emphasizes the need to continue the far-infrared spectroscopic field measurements under cold, very dry conditions.

Calculations of the radiative forcing due to a simultaneous doubling of CO_2, N_2O, and CH_4 have shown that differences in the radiative forcing calculations using the various HITRAN databases are small fractions of the total radiative forcing. Even the largest overall radiative forcing induced by differences among the HITRAN databases is considerably smaller than the range reported for the modeled radiative forcing estimates. Thus, the line parameter updates to the HITRAN database are not a significant source for discrepancies in the radiative forcing calculations appearing in the Intergovernmental Panel on Climate Change reports.

An inter-comparison between the flux calculations using the 1982 and 2004 HITRAN databases has shown that several of the thermal infrared intervals in the Fu and Liou model produce discrepancies that exceed the 1% accuracy achievable with correlated *k*-distribution models. Nevertheless, integration over the entire thermal infrared produces flux differences of order 1 $W\,m^{-2}$. Thus, upgrading the Fu and Liou correlated *k*-distribution coefficients, which are based on the 1982 HITRAN database, may not be necessary unless accuracies better than 1 $W\,m^{-2}$ are required.

Differences among the continuum formulations subsequent to the CKD 2.1 code tend to be comparable to the differences among the various HITRAN databases; however, use of the older RSB continuum formula produces significantly larger flux differences. Thus, replacement of the RSB continuum is warranted. Inclusion of line mixing for the Q-branches of CO_2 is a welcome addition to the HITRAN database; especially considering the significant impact that line mixing has upon satellite retrievals of CO_2 abundances and atmospheric temperature profiles, both of which are critical to understanding climate change effects.

Acknowledgments

The author would like to acknowledge the valuable advice and suggestions provided by R.A. Pertzborn, T.P. Charlock, M.G. Mlynczak, M.A.H. Smith, L.S. Rothman, and two anonymous reviewers. The author would also like to acknowledge the support provided by the Floyd L. Thompson Fellowship Program and the Science Mission Directorate through the Clouds and the Earth's Radiant Energy Systems and Far-Infrared Spectroscopy of the Troposphere projects.

References

[1] Forster P, Ramaswamy V, Artaxo P, Berntsen T, Betts R, Fahey DW, et al. Changes in atmospheric constituents and in radiative forcing. In: Solomon S, Qin D, Manning M, Chen Z, Marquis M, Averyt KB, Tignor M, Miller HL, editors. Climate change 2007: the physical science basis. Contribution of Working Group 1 to the Fourth Assessment Report of the Intergovernmental Panel on Climate Change. New York, NY: Cambridge University Press; 2007. p. 129–234.

[2] Ellingson RG, Ellis J, Fels S. The intercomparison of radiation codes in climate models: longwave results. J Geophys Res 1991;96(D5):8929–53.
[3] Tjemkes SA, Patterson T, Rizzi R, Shephard MW, Clough SA, Matricardi M, et al. The ISSWG line-by-line inter-comparison experiment. JQSRT 2003;77:433–53.
[4] Kratz DP, Mlynczak MG, Mertens CJ, Brindley H, Gordley LL, Martin-Torres J, et al. An inter-comparison of far-infrared line-by-line radiative transfer models. JQSRT 2005;90:323–41.
[5] Clough SA, Iacona MJ, Moncet J-L. Line-by-line calculations of atmospheric fluxes and cooling rates: application to water vapor. J Geophys Res 1992;97(D14):15761–85.
[6] Wiscombe WJ. Extension of the doubling method to inhomogeneous sources. JQSRT 1976;16:477–89.
[7] Fu Q, Liou KN. Parameterization of the radiative properties of cirrus clouds. J Atmos Sci 1993;50:2008–25.
[8] Rothman LS, Jacquemart D, Barbe A, Benner DC, Birk M, Brown LR, et al. The HITRAN 2004 molecular spectroscopic database. JQSRT 2005;96:137–204.
[9] Clough SA, Kneizys FX, Davies RW. Line shape and the water vapor continuum. Atmos Res 1989;23:229–41.
[10] Clough SA, Shephard MW, Mlawer EJ, Delamere JS, Iacono MJ, Cady-Pereira K, et al. Atmospheric radiative transfer modeling: a summary of the AER codes. JQSRT 2005;91:233–44.
[11] Collins WD, Ramaswamy V, Schwarzkopf, Sun Y, Portmann RW, Fu Q, et al. Radiative forcing by well-mixed greenhouse gases: estimates from climate models in the IPCC AR4. J Geophys Res 2006;111:D14317.
[12] Rothman LS, Gamache RR, Barbe A, Goldman A, Gillis LR, Brown LR, et al. AFGL atmospheric absorption line parameters compilation: 1982 edition. Appl Opt 1983;22:2247–56.
[13] Rothman LS, Gamache RR, Goldman A, Brown LR, Toth RA, Pickett HM, et al. The HITRAN database: 1986 edition. Appl Opt 1987;26:4058–97.
[14] Rothman LS, Gamache RR, Tipping RH, Rinsland CP, Smith MAH, Benner DC, et al. The HITRAN molecular database: editions of 1991 and 1992. JQSRT 1992;48:469–507.
[15] Rothman LS, Rinsland CP, Goldman A, Massie ST, Edwards DP, Flaud J-M, et al. The HITRAN molecular spectroscopic database and HAWKS (HITRAN Atmospheric Workstation): 1996 edition. JQSRT 1998;60:665–710.
[16] Rothman LS, Barbe A, Benner DC, Brown LR, Camy-Peyret C, Carleer MR, et al. The HITRAN molecular spectroscopic database: edition of 2000 including updates of 2001. JQSRT 2003;82:5–44.
[17] Tobin DC, Revercomb HE, Knuteson RO, Lesht BM, Strow LL, Hannon SE, et al. Atmospheric radiation measurement site atmospheric state best estimates for atmospheric infrared sounder temperature and water vapor retrieval validation. J Geophys Res 2006;111:D09S14.
[18] Fu Q, Liou KN. On the correlated *k*-distribution method for radiative transfer in nonhomogeneous atmospheres. J Atmos Sci 1992;49:2139–56.
[19] Pinnock S, Shine KP. The effects of changes in HITRAN and uncertainties in the spectroscopy on infrared irradiance calculations. J Atmos Sci 1998;55:1950–64.
[20] Rothman LS, Hawkins RL, Wattson RB, Gamache RR. Energy levels, intensities, and linewidths of atmospheric carbon dioxide bands. JQSRT 1992;48:537–66.
[21] Flaud J-M, Camy-Peyret C, Rinsland CP, Smith MAH, Devi VM. Atlas of ozone spectral parameters from microwave to medium infrared. San Diego, CA: Academic Press; 1990. p. 1–35.
[22] Kratz DP, Chou M-D, Yan M-H, Ho C-H. Minor trace gas radiative forcing calculations using the *k* distribution with one-parameter scaling. J Geophys Res 1998;103(D24):31647–56.
[23] Kratz DP, Rose FG. Accounting for molecular absorption within the spectral range of the CERES window channel. JQSRT 1999;61:83–95.
[24] Kratz DP. High resolution modeling of the far-infrared. Proc SPIE 2001;4485(34):171–80.
[25] Kratz DP, Priestley KJ, Green RN. Establishing the relationship between the CERES window and total channel measured radiances for conditions involving deep convective clouds at night. J Geophys Res 2002;107(D15):4245.
[26] McClatchey RA, Fenn RW, Selby JE, Volz FE, Garing JS. Optical properties of the atmosphere, 3rd ed., AFCRL-72-0497, Environmental Research Papers no. 411. Bedford, MA: Air Force Cambridge Research Laboratory; 1972.
[27] Aumann HH, Chahine MT, Gautier C, Goldberg MD, Kalnay E, McMillin LM, et al. AIRS/AMSU/HSB on the Aqua mission: design, science objectives, data products, and processing systems. IEEE Trans Geosci Remote Sensing 2003;41(2):253–64.
[28] Mlynczak MG, Johnson DG, Latvakoski H, Jucks K, Watson M, Kratz DP, et al. First light from the Far-Infrared Spectroscopy of the Troposphere (FIRST) instrument. Geophys Res Lett 2006;33:L07704.
[29] Tobin DC, Best FA, Brown PD, Clough SA, Dedecker RG, Ellingson RG, et al. Downwelling spectral radiance observations at the SHEBA ice station: water vapor continuum measurements from 17 to 26 μm. J Geophys Res 1999;104(D2):2081–92.
[30] Baum BA, Frey RA, Mace GG, Harkey MK, Yang P. Nighttime multilayered cloud detection using MODIS and ARM data. J Appl Meteorol 2003;42:905–19.
[31] Mlynczak MG, Harries JE, Rizzi R, Stackhouse PW, Kratz DP, Johnson DG, et al. The far-infrared: a frontier in remote sensing of Earth's climate and energy balance. Proc SPIE 2001;4485(34):150–8.
[32] Mlynczak M.G., Johnson D, Bingham G, Jucks K, Traub W, Gordley L, et al. In: The far-infrared spectroscopy of the troposphere (FIRST) project, Proceedings of the IEEE international geosciences and remote sensing symposium, vol. 1, 2003. p. 512–4.
[33] Wielicki BA, Barkstrom BR, Harrison EF, Lee RB, Smith GL, Cooper JE. Clouds and the Earth's Radiant Energy System (CERES): an earth observing system experiment. Bull Am Meteorol Soc 1996;77:853–68.

[34] Charlock TP, Rose FG, Rutan DA, Jin Z, Kato S. The global surface and atmospheric radiation budget: an assessment of accuracy with 5 years of calculations and observations. In: Proceedings of the 12th conference on atmospheric radiation, Madison, WI, 10–14 July 2006.
[35] Lacis A, Oinas V. A description of the correlated *k*-distribution method for modeling nongray gaseous absorption, thermal emission, and multiple scattering in vertically inhomogenous atmospheres. J Geophys Res 1991;96(D5):9027–63.
[36] Roberts RE, Selby JEA, Biberman LM. Infrared continuum absorption by atmospheric water vapor in the 8–12 micrometer window. Appl Opt 1976;15:2085–90.
[37] Rodriques R, Jucks KW, Lacome N, Blanquet G, Walrand J, Traub WA, et al. Model, software, and database for computation of line-mixing effects in infrared Q branches of atmospheric CO_2: I. Symmetric isotopomers. JQSRT 1998;61:153–84.
[38] Jucks KW, Rodriques R, Le Doucen R, Claveau C, Traub WA, Hartmann J-M. Model, software, and database for computation of line-mixing effects in infrared Q branches of atmospheric CO_2: II. Minor and aymmetric isotopomers. JQSRT 1999;63:31–48.
[39] Salomonson VV, Barnes WL, Maymon PW, Montgomery HE, Ostrow H. MODIS—advanced facility instrument for studies of the Earth as a system. IEEE Trans Geosci Remote Sensing 1989;27(2):145–53.
[40] Strow LL, Tobin DC, Hannon SE. A compilation of first-order line-mixing coefficients for CO_2 Q-branches. JQSRT 1994;52:281–94.